

SCIENTIFIC REPORTS

OPEN

LIM Protein Ajuba associates with the RPA complex through direct cell cycle-dependent interaction with the RPA70 subunit

Sandy Fowler^{1,2}, Pascal Maguin^{1,3}, Sampada Kalan^{1,2,4} & Diego Loayza^{1,2} 

DNA damage response pathways are essential for genome stability and cell survival. Specifically, the ATR kinase is activated by DNA replication stress. An early event in this activation is the recruitment and phosphorylation of RPA, a single stranded DNA binding complex composed of three subunits, RPA70, RPA32 and RPA14. We have previously shown that the LIM protein Ajuba associates with RPA, and that depletion of Ajuba leads to potent activation of ATR. In this study, we provide evidence that the Ajuba-RPA interaction occurs through direct protein contact with RPA70, and that their association is cell cycle-regulated and is reduced upon DNA replication stress. We propose a model in which Ajuba negatively regulates the ATR pathway by directly interacting with RPA70, thereby preventing inappropriate ATR activation. Our results provide a framework to further our understanding of the mechanism of ATR regulation in human cells in the context of cellular transformation.

Cells possess conserved mechanisms that have evolved to sense, respond to and repair specific types of DNA damage¹. These pathways are intimately linked to checkpoint systems and represent highly coordinated and complex responses to extrinsic or intrinsic damage¹. Of those, the ATR pathway responds to DNA replication stress, such as nucleotide imbalance or collapsed forks, or accumulation of single stranded DNA which are events occurring, albeit to a low degree, at each and every S phase of the cell cycle^{2,3}. Importantly, the ATR pathway is a tumor suppressor system acting early in tumorigenesis and cell transformation². Many aspects of ATR activation have been extensively characterized, involving the accumulation of single stranded DNA binding complex RPA, the phosphorylation on the N-terminus of the RPA32 subunit⁴, and further recruitment of the 9-1-1 complex, TOPBP1 and ATR-ATRIP, which are factors necessary for the activation of ATR kinase activity that assemble on the RPA70 subunit⁵⁻⁷. The ATR kinase phosphorylates substrates that orchestrate cell cycle pausing and damage repair, such as Chk1 or Claspin. Local recruitment of ATR on RPA includes autophosphorylation at Ser198⁸, an event that is also required for activation of the pathway. The resulting effects lead to a pause in the cell cycle during S phase, through phosphorylation and activation of Chk1 and Cdc25A, or in some cases apoptosis, through activation of Cdc25C.

RPA plays a crucial role in the ATR activation pathway. RPA is a trimeric complex composed of the three subunits RPA70, RPA32 and RPA14⁹. This complex constitutes an important single stranded DNA binding complex, which binds DNA with high affinity¹⁰ (and ref. therein). DNA binding is mediated by specific domains in RPA70 and RPA32, which adopt a structural pattern called OB-fold (for oligosaccharide/oligonucleotide binding)^{11,12}. The trimeric RPA complex possesses six such OB folds, with RPA70 (4), RPA32 (1) and RPA14 (1). The RPA14 subunit is essential for stability of the complex¹². The N-terminal OB fold in RPA70 (termed RPA70N⁶) represents a platform for the assembly of RAD9 and ATRIP-ATR, necessary for the recruitment of TOPBP1, the activator of ATR kinase^{6,13}. RPA is essential for DNA replication, by allowing fork progression and lagging strand synthesis, for recombination, by catalyzing strand invasion, and DNA repair, by being involved, among other activities, in ATR activation. In DNA repair, RPA possesses both structural and signaling roles. The complex has a structural

¹Department of Biological Sciences, Hunter College, 695 Park Avenue, New York, NY, 10065, USA. ²CUNY Graduate Center, Ph.D. program in Molecular, Cell and Developmental Biology, 365 Fifth Avenue, New York, NY, 10016, USA. ³Present address: The Rockefeller University, 1230 York Avenue, New York, NY, 10021, USA. ⁴Present address: Department of Oncological Sciences, Icahn School of Medicine at Mount Sinai, One Gustave L. Levy Place, New York, NY, 10029, USA. Correspondence and requests for materials should be addressed to D.L. (email: diegol@genectr.hunter.cuny.edu)

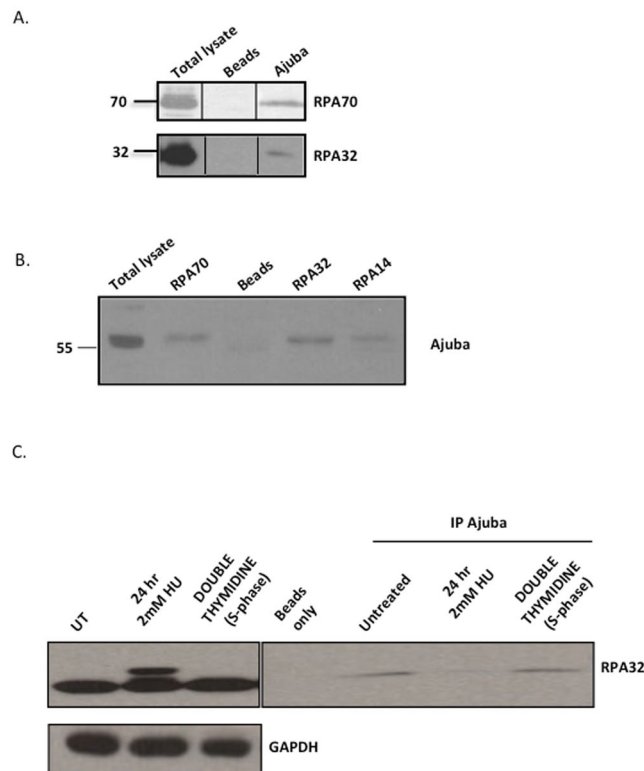


Figure 1. Ajuba is in association with the RPA complex, and dissociates upon hydroxyurea treatment. **(A)** IP-Western on immunoprecipitations with Ajuba serum from HTC75 total extracts. The blots were probed with the indicated RPA antibodies. **(B)** IP-Western using the indicated RPA antibodies for immunoprecipitations, and blotted for Ajuba. **(C)** IP-Western using anti-Ajuba antibodies for immunoprecipitations, and blotted for RPA32. Total extracts shown on the left panel. Cells were untreated (control), treated with 2 mM hydroxyurea (HU) for 24 hr, or synchronized by double Thymidine block and released for 2 hr. See also Figures S1, S3 and S4 for data with IMR90 cells. Panels shown are cropped from full-length blots shown in Supplemental Figure S9.

role given its ability to bind single stranded DNA, thereby preventing secondary structures incompatible with replication or repair, and a signaling role related to the assembly of the ATR activation complex on RPA70N. We have previously implicated the LIM (LIN-1, ISL-1, MEC-1) domain protein Ajuba as a new player in the ATR pathway¹⁴. The LIM superfamily of proteins, constituted by 60 members in the human proteome, is subdivided into seventeen families, all with predicted LIM domains in various arrangements^{15,16}. LIM domains are known protein interaction domains that present distinctive loops defined by interactions between Cysteine and Histidine residues coordinating a Zn^{++} ion¹⁶. Ajuba itself is part of the Zyxin family, which in addition includes TRIP6 and LPP, two components that are involved in telomere protection, through binding of the OB fold protein POT1^{17,18}. The Zyxin family is characterized by the presence of three C-terminal LIM domains¹⁶. We have shown that Ajuba acts as a negative regulator of ATR in unperturbed cells¹⁴. Notably, upon depletion of the protein, cells experience S phase delay along with strong activation of Chk1, a known ATR substrate, and undergo apoptosis. Our current model is that Ajuba exerts an inhibitory activity to full-blown activation of the ATR kinase, and is essential to prevent cell death by apoptosis in unperturbed cells. This inhibitory effect correlates with our observation that Ajuba associates with the RPA complex in the cell¹⁴, and thus associates with a core component of early ATR activation. In this study, we show that the interaction between Ajuba and the RPA complex is direct and occurs through the RPA70 subunit. We found that this association occurs in the nucleus, and that the amounts of Ajuba along with the degree of co-localization between Ajuba and RPA are increased in S phase, suggesting cell cycle-dependent regulation of the localization of Ajuba, and perhaps of its interaction with RPA as well. We show that hydroxyurea, known to induce DNA replication stress and activation of ATR, leads to dissociation of Ajuba from RPA and to efficient export of Ajuba from the nucleus. Based on our findings, we propose a model for Ajuba in preventing inappropriate ATR induction during S phase.

Results

Ajuba associates with the RPA complex and dissociates upon replication stress. In order to determine whether Ajuba exhibits association with the whole RPA complex, or to a particular subunit of RPA, co-immunoprecipitations were performed with HTC75 cell extracts using antibodies to each subunit separately. As seen in Fig. 1A, Ajuba is able to immunoprecipitate RPA70 or RPA32 in separate immunoprecipitations. In addition, antibodies to each of the three RPA subunits are able to pull down Ajuba independently (Fig. 1B). This suggests that Ajuba associates in cells not with one of the RPA subunits separately, but with the whole RPA

complex. In each case, the estimate of the pull down efficiency is between 2 and 5% of total RPA in association with Ajuba (see Materials and Methods). Therefore, a small pool of RPA is involved in the association. In turn, a small fraction of Ajuba is in association with the RPA complex. Therefore, the interaction is robust but involves a small fraction of either partner.

Our previous studies showed that depletion of Ajuba led to an apparent activation of ATR in otherwise unperturbed cells¹⁴. We asked whether the enforcement of the ATR response through DNA replication stress induced by hydroxyurea treatment had an effect on the association. We found that treating cells with 2 mM hydroxyurea led to a significant reduction in the association of Ajuba and RPA, as observed by the amounts of RPA32 precipitated by anti-Ajuba antibodies (Fig. 1C, right panel). The activation of the DNA damage response is evident from the induction of phosphorylation of RPA32 (1C, left panel). Hydroxyurea also reduced the amount of RPA70 precipitating with anti-Ajuba antibodies (Fig. S1), arguing for a dissociation of Ajuba with the whole RPA complex under conditions of replication stress. In addition, the overall amounts of Ajuba are unchanged during hydroxyurea treatment (Fig. S2), showing that the decrease in the amounts of Ajuba is not due to a reduction in protein stability. Since hydroxyurea treatment influences the cell cycle profile in culture, by enriching for cells in S phase (Fig. S3), we asked whether the dissociation of Ajuba and RPA was a result of cell cycle stage. We therefore synchronized cells in G1 through a double thymidine block, released the cells in S phase and probed for possible Ajuba-RPA dissociation (Fig. 1C, right panel). We found no perceptible effect on the amount of Ajuba associated with RPA in S phase cells, and concluded that the dissociation seen upon hydroxyurea treatment was not merely due to delay in S phase, and therefore was the consequence of DNA replication stress. Finally, the association of Ajuba with RPA and the effect of hydroxyurea are not a specific cell-line or tumor phenotype, since the same observations were made in IMR90 cells, a normal diploid human fibroblast cell line (Figs S1, S3, S4).

Ajuba nuclear localization is cell cycle regulated, and is significantly increased in S phase.

Whereas the RPA complex is localized in the nucleus, Ajuba possesses a complex intracellular trafficking: as other members of the Zyxin LIM family, it is mostly present in the cytoplasm, where it is involved in cell-cell and cell-matrix adhesion, and is actively shuttled in and out of the nucleus by virtue of a discernible nuclear export sequence (NES). Thus, a small pool of Ajuba (about 10%, S.K. and D.L., unpublished) is present at steady state in the nucleus. Given the dynamic trafficking of Ajuba, and our observation that it controls ATR activation in S phase, we probed whether the localization of Ajuba was dependent on the cell cycle. In unsynchronized cells, about 33% of the cells showed a clear nuclear staining pattern for Ajuba in HTC75 and IMR90 cells, as shown in Fig. S5A. In those, the staining pattern for Ajuba exhibited clearly distinguishable foci, overlaid on an overall diffuse nuclear staining pattern. In cells synchronized and released in S phase, we found a clear increase in the fraction of cells containing nuclear Ajuba (Fig. 2): the percentage increased from 33% at time of release to 68.9% at the 4-hr time point, corresponding to mid-S phase, and was followed by a decrease to 46.8% at the 6 hr time point (Fig. 2). We confirmed this observation by assessing whether nuclear Ajuba was found in replicating cells, which are visualized by BrdU incorporation (Fig. 3). We found that at the 4-hour time point, with 81.4% of BrdU-positive cells, over 65% of the cells contained nuclear Ajuba with 3 or more foci of co-localization. Thus, it appeared that Ajuba was found in higher amounts in cells undergoing S phase, with some of the signal displaying a punctate staining pattern. We conclude that Ajuba presents a significant increase in nuclear accumulation occurs during S phase. This increase could occur through a combination of effects on the flow of nuclear import, and the efficiency of NES-mediated export. We do believe that nuclear export is an important step because of the observation that Leptomycin B, an inhibitor of CRM1-mediated export and known to lead to nuclear accumulation of Ajuba²⁰, leads to a significant increase in its co-localization with RPA70 (up to 59.3%, see Fig. S5B).

Ajuba partially co-localizes with RPA in the nucleus, with co-localization increased in S phase.

To address whether Ajuba-RPA interaction takes place in the nucleus, we performed co-immunofluorescence for both proteins in HTC75 and IMR90 cells. We found a significant degree of co-localization in the nucleus, in unsynchronized cells (Fig. S5A). The co-localization was observed specifically with the Ajuba signal that was found in foci, and only in a subpopulation of cells. Given our result that Ajuba appeared enriched in S phase nuclei, we asked whether the co-localization between Ajuba and RPA occurred primarily in S phase. We therefore repeated the experiment with cells released in S phase, and found that the percentage of nuclei exhibiting more than 3 nuclear foci for both Ajuba and RPA70 greatly increased up to mid S phase (4 hr time point), from 17.6% to 61.9%, then decreased to 27.4% (6 hr time point) (Fig. 4). Again, cells in G1 (0 hr) did exhibit some level of co-localization (17%), but to a lesser degree compared to unsynchronized cells (17.6% versus 27.5%). Thus, the amounts of Ajuba and degree of association with the RPA complex are not exclusive to S phase, but appear to be highly enriched at an interval representing early to mid-S phase. In each nucleus, the degree of co-localization in foci was not complete, indicating that some sites containing Ajuba remain to be identified. We looked at the possibility of co-localization between Ajuba and PCNA, essential for lagging strand synthesis. We did find significant co-localization between Ajuba and PCNA as well (Fig. S6A). Significant co-localization between nuclear Ajuba and BrdU was also observed in a fraction of the cells, mostly in S phase (Fig. 3) but also in a small fraction of unsynchronized cells (Fig. S6B). It is therefore possible that some of the nuclear Ajuba foci represent sites of active DNA replication.

Ajuba interacts with the RPA70 subunit directly. We have documented previously an interaction between Ajuba and RPA by co-immunoprecipitation¹⁴, which does not necessarily imply a direct contact. Since the association between Ajuba and the RPA complex could be indirect and mediated by additional factors, or direct through a specific protein-protein interaction, we investigated whether a direct protein contact could be detected between Ajuba and one of the RPA subunits. To this end, the *in vitro* translation system using rabbit reticulocyte lysates was employed to address the nature of interaction between Ajuba and RPA. Each of the RPA subunit was cloned into pCMVTnT vector and Ajuba was cloned into a N-terminal His-tagged vector (pcDNA

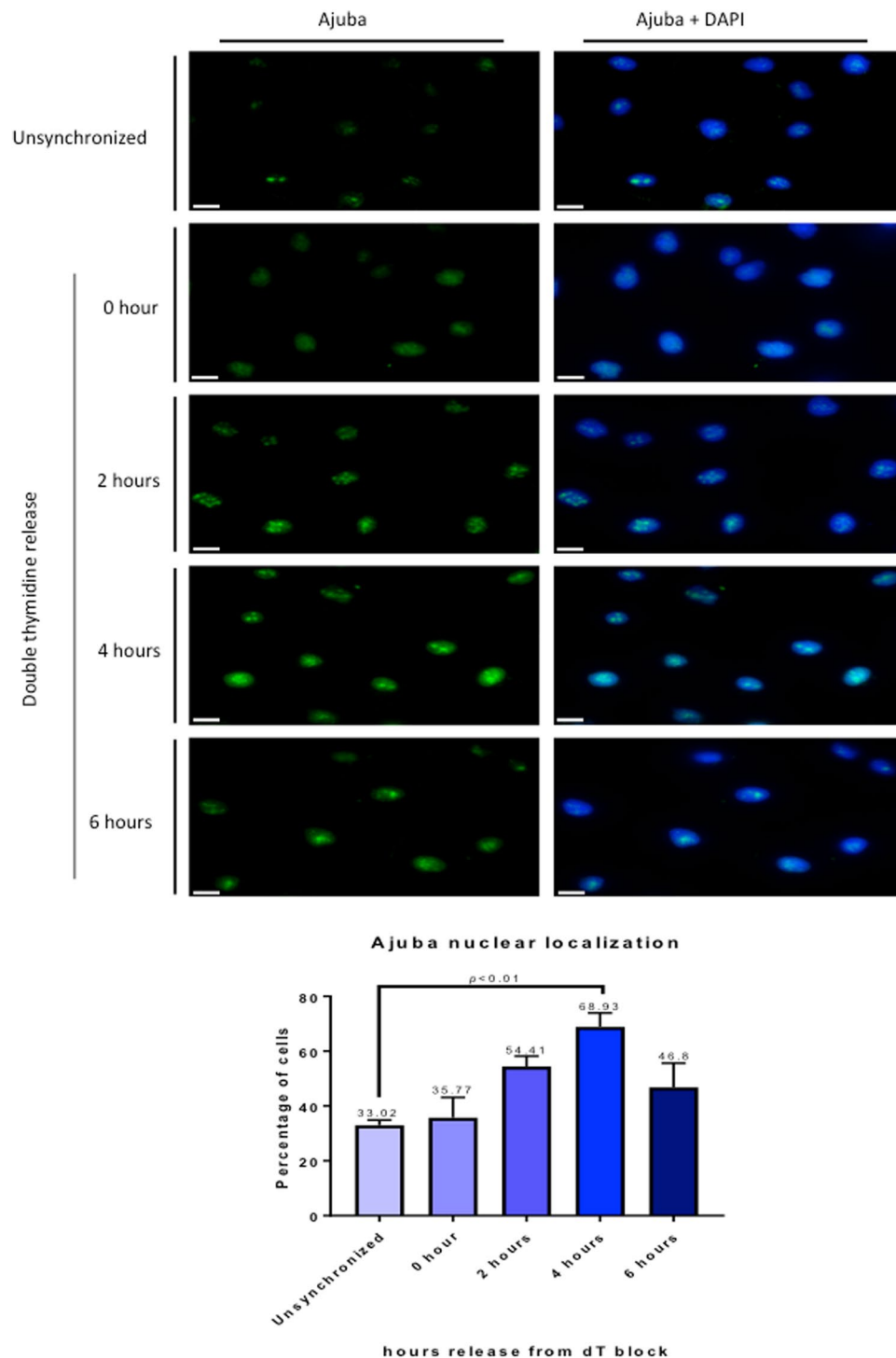


Figure 2. Ajuba nuclear localization is increased during S phase. HTC75 cells were synchronized to G1/S border with double thymidine block and released into S phase, with cells processed for IF at the indicated time points. (Top) Immunofluorescence of Ajuba in unsynchronized and synchronized cells. (Bottom) Quantitation of cells positive for nuclear Ajuba at each time point ($n = 100$).

3.1/His B). Ajuba was co-translated with each of the RPA subunits separately and the reaction mixtures were subjected to His-tag pulldown using nickel beads. As shown in Fig. 5A, Ajuba was found to pull down with the large subunit of the RPA complex, RPA70. Quantitative analysis of pull down efficiencies showed that 61.9% of the *in vitro* translated RPA70 was precipitated by HIS-Ajuba, with RPA32 yielding only background (13%) (Fig. 5B). As a control, we probed whether Ajuba could associate with POT1, the OB fold telomeric single strand binding protein. There was no detectable binding between the two (Fig. S7A). Our data indicate that there is a direct and specific contact between Ajuba and the RPA complex, through the RPA70 subunit.

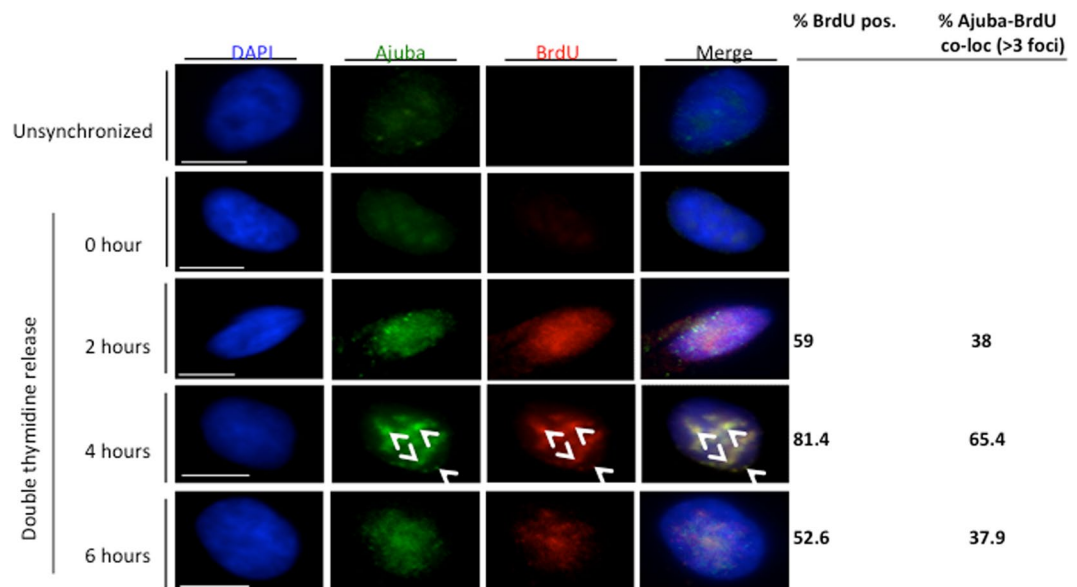


Figure 3. Nuclear Ajuba is found primarily in BrdU-positive cells. HTC75 cells were synchronized, then released in BrdU-containing medium. The BrdU was washed off after 1 hour. Cells were co-stained for Ajuba and BrdU at the indicated time points. The percent of nuclei with >3 foci of co-localization is shown (bottom right).

Direct contact between RPA70 and Ajuba is mediated by OB fold A of RPA70 and the central region of Ajuba.

The Ajuba-RPA70 interaction prompted us to further define the region on both proteins that mediate this interaction. In order to map the region of interaction, truncation alleles of RPA70 were generated by PCR and cloned into pCMVtnT vector. The N-terminus of RPA70, OB fold F, has been extensively studied for its function as an “interaction hub” with proteins involved in DNA damage and checkpoint response⁶. In the central region of RPA70, OB folds A and B have been shown to associate with proteins involved in DNA replication and repair. At the C-terminus, OB fold C was shown to be involved in subunit interaction¹². Truncations were constructed based on previous sequence and structural analysis, hence separating RPA70 into OB fold F and OB folds A-B-C. The alleles were co-translated with His-tagged full-length Ajuba and the reaction mixtures were subjected to His-tag pull downs.

Figures 6 and 7A show the pull downs between full-length Ajuba and different RPA70 truncations as shown, and the quantification of the pull down efficiency of each allele. OB folds A-B-C was found to pull down with full-length Ajuba with a yield very similar to full-length RPA70 (Fig. 6A). When half of OB fold A was truncated, the pull down with full-length Ajuba was decreased to 58.7%, with full-length RPA70 being set at 100% (Figs 6B, 7A). OB fold F, as well as an allele containing only OB folds B and C, showed minimal binding activity with full-length Ajuba (Figs 7A, S7B). Taken together, Ajuba physically contacts OB ABC of RPA70 and not OB F *in vitro*. In particular, OB fold A seemed to be the most important region for the interaction.

We attempted to test whether OB fold A was sufficient for the interaction by testing an allele fusing OB fold A with OB fold F. Since OB F did not exhibit interaction with Ajuba, any binding activity would be ascribed to OB fold A. Surprisingly, OB F + A did not exhibit any major increase in binding with Ajuba compared to OB F alone (Fig. 7A). Collectively, our data suggests that OB A is necessary but not sufficient for the interaction with Ajuba, and possibly other domains in RPA70 are required to reconstitute full binding activity.

We also sought to identify interaction domains in Ajuba. A previous study has described the preLIM region by itself localized in the cytoplasm, and LIM domains bearing a determinant for nuclear localization^{19,20}. This prompted construction of alleles containing the preLIM region and LIM domains, and probed for RPA70 interaction. Each allele was co-translated with full-length RPA70 and subjected to binding assays with nickel beads. Figure 6C,D show that both Ajuba alleles exhibit very low binding activity.

We hypothesized that the actual binding domain in Ajuba was severed in our initial constructs, and might lie between the pre-LIM and LIM regions. We then constructed additional alleles with different end points, specifically harboring the preLIM region with adjacent LIM domains (LIM 1 and 2) in order to preserve the central region. As shown in Figs 6D and 7A, the pull down signal of full-length RPA70 increased when LIM domain 1 or LIM domains 1 and 2 are added to the preLIM region. Quantitation of RPA70 pull-down efficiency by Ajuba mutants (Fig. 7B) shows a significant decrease in binding activity in all mutants compared to full-length Ajuba, with pre-LIM + LIM1 being the most efficient at 45.3% of full-length (Fig. 7B), once again arguing that no single domain could account for the full binding activity of the protein. In addition, preLIM-LIM1 and preLIM-LIM1-LIM2 constructs exhibited higher pull down efficiencies than either preLIM region or LIM domains alone. This suggests that the central region of Ajuba participates in this physical contact with RPA70, along with other possible motifs. Our model, then, is that the central portion in Ajuba, between residues 337 and 397, mediates a direct interaction with OB fold A of RPA70, between residues 169 and 300. Our model for this interaction is shown in Fig. S8.

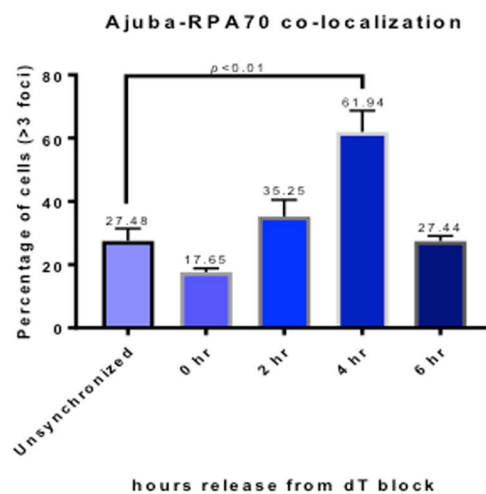
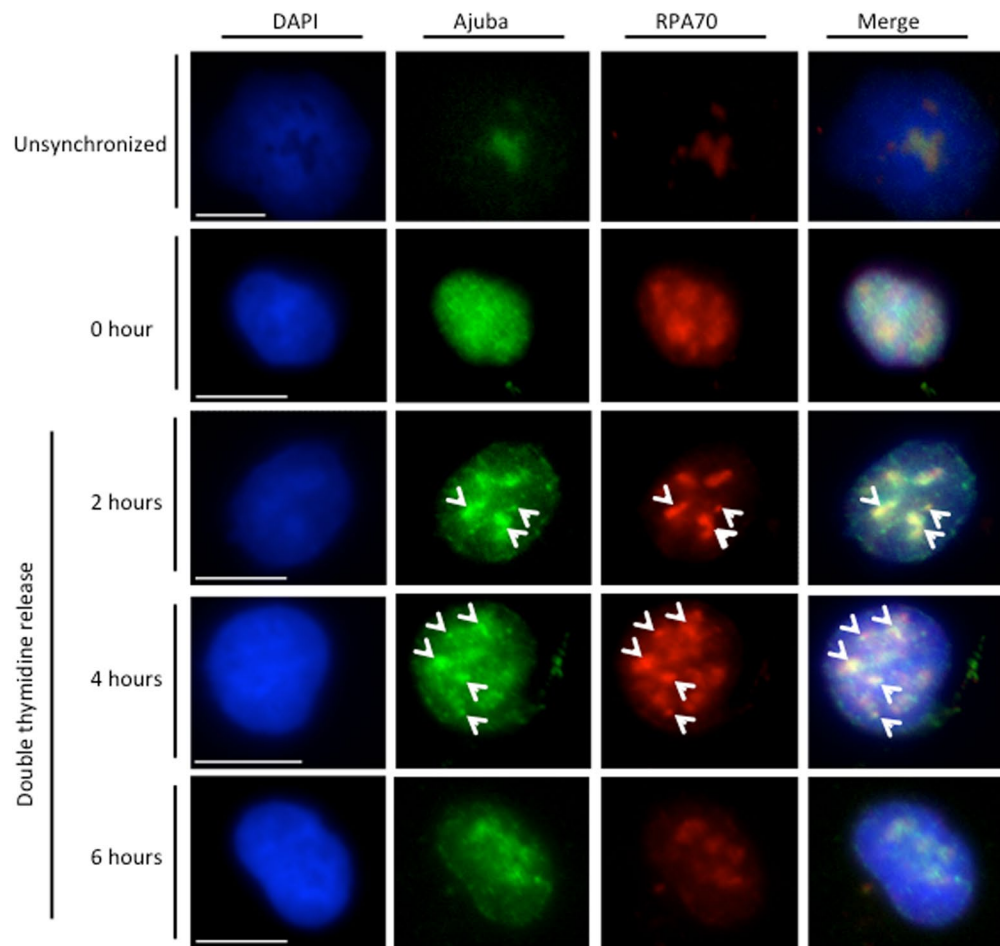
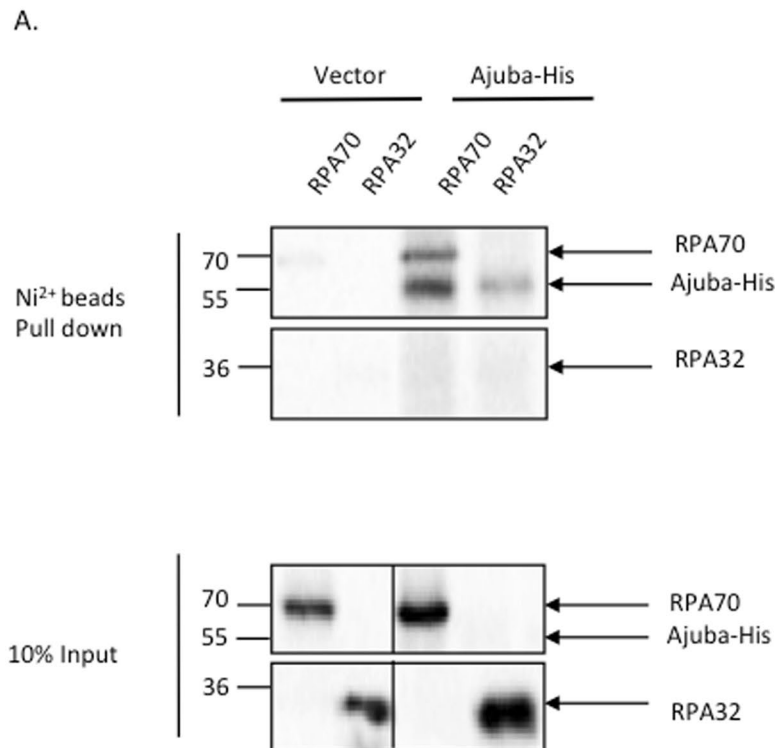


Figure 4. Increase of Ajuba-RPA70 co-localization in the nucleus during S phase. HTC75 cells were synchronized to G1/S border with double thymidine block and released into S phase with cells processed for IF at the indicated time points. (Top) Co-immunofluorescence of Ajuba and RPA70 in unsynchronized and synchronized cells. Arrowheads point to sites of co-localization (Bottom) Quantitation of cells exhibiting >3 foci of Ajuba-RPA70 co-localization in the nucleus at each time point ($n = 100$).

Hydroxyurea leads to significantly diminished nuclear accumulation of Ajuba. The decreased association of Ajuba with RPA in cells experiencing DNA replication stress, combined with the enrichment of Ajuba in S phase nuclei prompted us to ask whether hydroxyurea could influence the intracellular localization of Ajuba: possibly, the dissociation of Ajuba from RPA could lead to active export in conditions of ATR activation.



B.

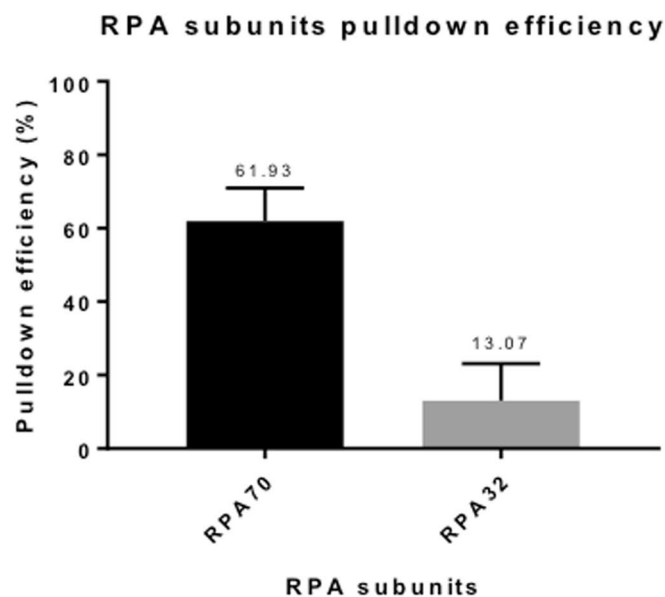


Figure 5. Ajuba can bind directly to the RPA70 subunit *in vitro*. *In vitro* co-translation of His-tagged Ajuba (Ajuba-His) and RPA subunits: RPA70, RPA32, and RPA14 (not shown) using rabbit reticulocyte lysates. **(A)** Autoradiography of affinity pull-down with Ajuba-His and co-translated RPA subunit. **(B)** Pull down efficiency (%) of each RPA subunit by Ajuba-His. Pull down efficiencies were determined by the quantification of pull down signal in autoradiography and normalized to input signal and the number of methionine of each construct. See Materials and Methods for further details. Panels are cropped from full-length PhosphorImager scans shown in Supplemental Figure S10.

Cells were treated with 2 mM hydroxyurea for 24 hr and the localization of Ajuba was assessed. We found that the nuclear accumulation of Ajuba was greatly reduced, from 38% in controls to 16.7% in cells treated with 2 mM hydroxyurea (Fig. 8). The concomitant change in the staining pattern of RPA 70 in 2 mM hydroxyurea confirmed

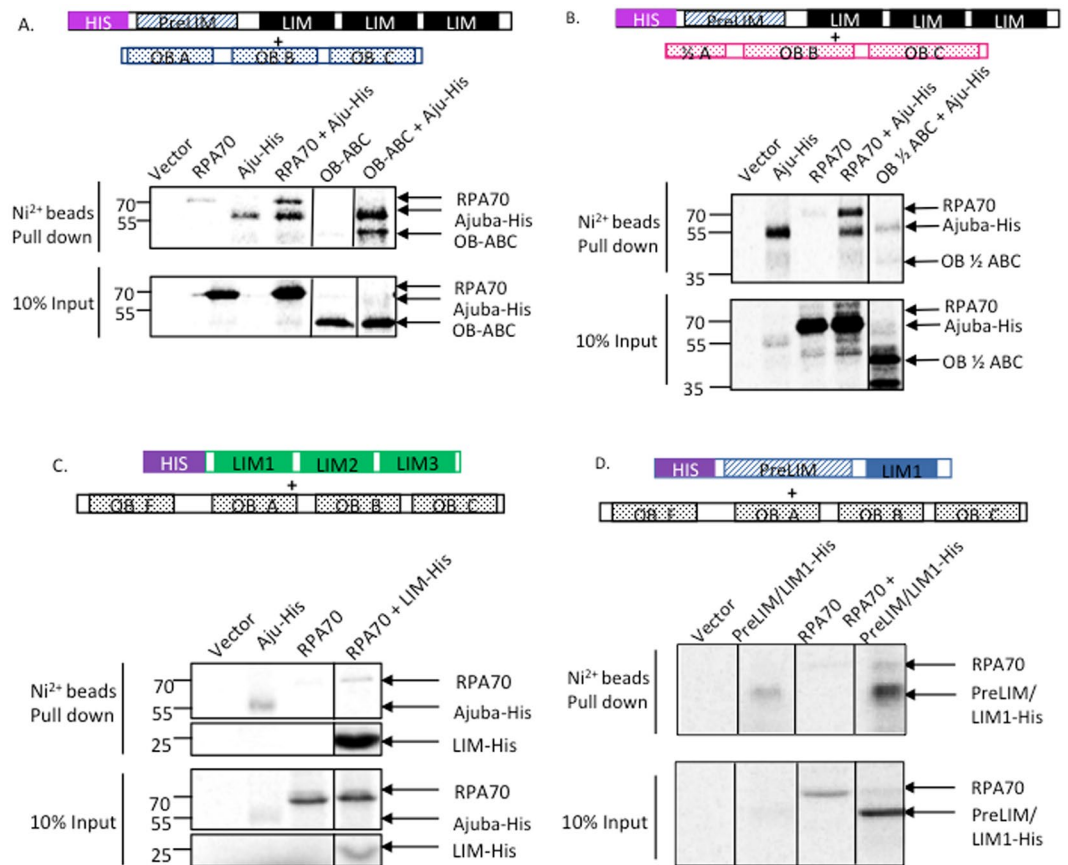


Figure 6. RPA70 OB fold A and Ajuba LIM domain 1 are important, but not sufficient, for the Ajuba-RPA70 interaction *in vitro*. Autoradiography of His tag pull downs with nickel beads in Ajuba/RPA70 mutants co-translations. (A) Deletion of OB fold F does not impact pull down with full-length Ajuba-His. (B) Truncation of half of OB fold A reduced pull down with full-length Ajuba-His. (C) LIM 1-2-3 pulls down full-length RPA70. (D) Addition of LIM domain 1 to the preLIM region enhanced pull down of full-length RPA70. Panels 6 A and 6B shown are cropped from full-length scans shown in Supplemental Figures S11, and in S13 for panel 6C. Panels are cropped from full-length PhosphorImager scans shown in Supplemental Figure S11 (A,B), S12 (C) and S13 (D).

the induction of DNA replication stress in nuclei with lowered Ajuba accumulation. Altogether, our data suggest that DNA replication stress leads to dissociation of Ajuba from RPA and active export from the nucleus.

Discussion

A number of studies have established a well-understood molecular pathway for ATR activation: stabilization of RPA on single stranded DNA, present in excess to normal amounts produced by the replication forks in S phase, leads to the assembly of a recruitment complex on the N-terminal OB fold of RPA70 (called OB-F or RPA70N)^{6,7}. The RPA70 subunit, therefore, represents a platform onto which RAD9, part of the activation 9-1-1 complex (RAD9-RAD1-HUS1), TopBP1 and ATR-ATRIP are recruited, leading to autophosphorylation of ATR and induction of the kinase⁸. While the assembly of the ATR activation complex can occur *in vitro* in a purified system, little is known about how ATR activation is prevented from occurring under non-inducing conditions. We have proposed, based on an earlier study, that Ajuba plays an important role in this context¹⁴. Given the observations that depletion of Ajuba leads to the induction of ATR in absence of any damage or causative agent, we have proposed that Ajuba acts as an inhibitor of ATR induction. We have also discovered that Ajuba associates with RPA, placing it at the core of ATR activation. Here, we show that the association between Ajuba and RPA is direct, through a contact with RPA70, and that, in cells, activation of ATR by hydroxyurea leads to dissociation of Ajuba from RPA accompanied by a strong reduction in nuclear accumulation. Our view is that the ATR activation complex is poised for assembly on the RPA70 recruitment platform, and that Ajuba must be dissociated from RPA for activation to occur. Whether Ajuba acts specifically in S phase remains to be determined, but our data suggest that its activity is especially important for S phase progression, given that depletion of the protein eventually leads to strong apoptotic signals, with the remaining cells being mostly delayed in S phase.

Ajuba has been described in a different setting, in maintaining the structure of desmosomes at cell adhesion sites²¹. Indeed, the majority of the protein is extra-nuclear, with only a small fraction (10% or less) present in the nucleus, and this in a small subset of the cells (SK and DL, unpublished, this study). Ajuba and other members

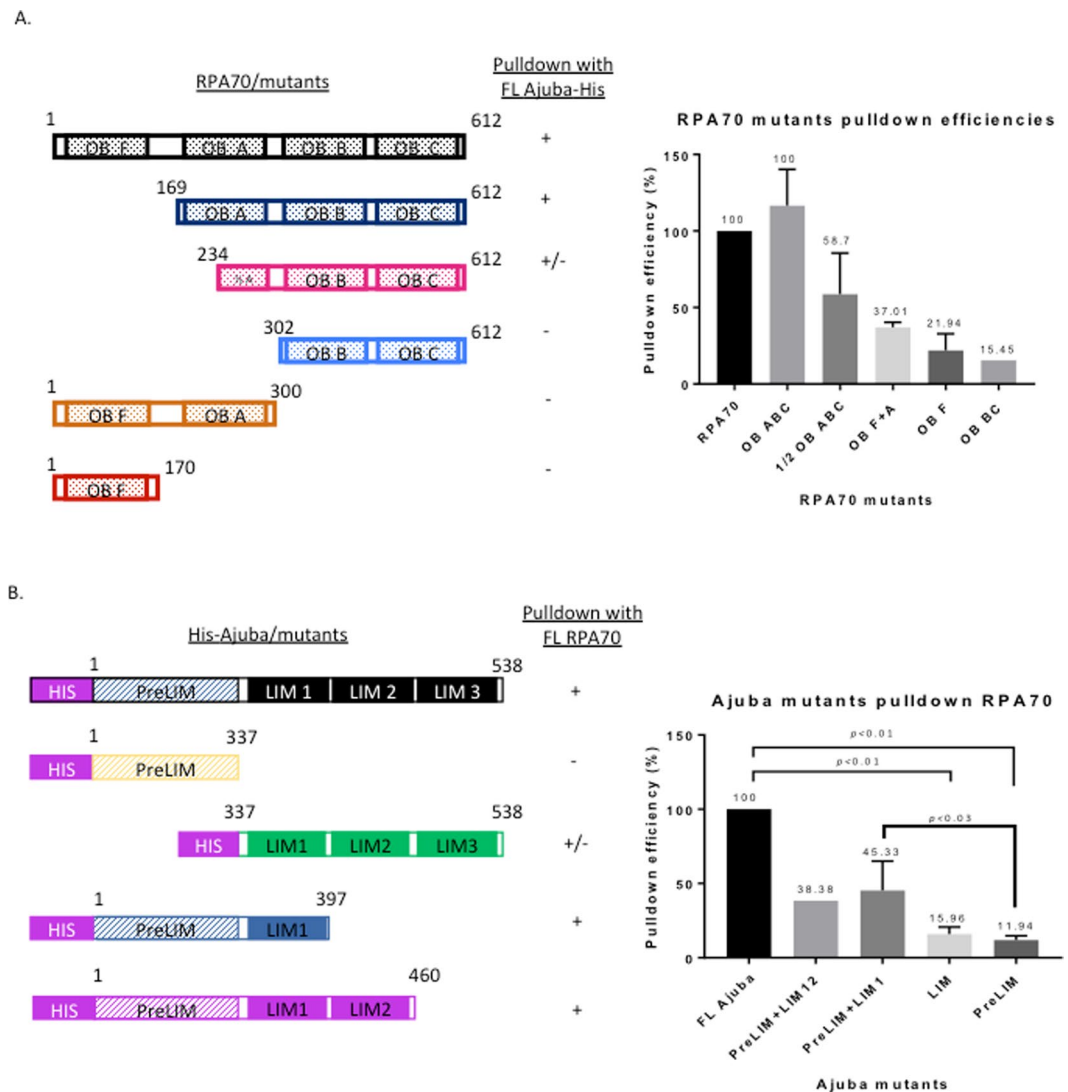


Figure 7. RPA70 and His-tagged Ajuba truncation allele constructs and pull-down efficiencies *in vitro*. (A) (Left) Full-length RPA70 and truncation constructs. (Right) Pull down efficiencies of each RPA70 by full-length Ajuba-His. (B) (Left) Full-length Ajuba-His and His-tagged truncation constructs. (Right) Pull down efficiencies of full-length RPA70 by each His-tagged Ajuba truncation allele.

of the Zyxin subfamily (Zyxin, TRIP6, LPP) are known to undergo a dynamic intracellular life cycle, with active shuttling in and out of the nucleus²² (see our model, Fig. 9). Export from the nucleus is an important part of this life cycle, because interfering with nuclear export leads to significant protein accumulation in the nucleus^{23,24}. Based on our results, the pool of Ajuba present in the nucleus could be maintained there through direct binding to RPA70, in the context of ATR inhibition (Fig. 9). Whether the intra- and extra- nuclear roles of Ajuba are linked and pertain to some kind of subcellular signaling remains to be determined, and separation-of-function alleles would be informative in this regard. Our work represents a first step in the design of such alleles. Once DNA damage has occurred, Ajuba could dissociate from RPA70 leading to active NES-dependent export out of the nucleus, possibly by “unmasking” of this motif following dissociation.

Our model put forth previously¹⁴ proposed that Ajuba prevents activation of ATR under non-inducing conditions, activation which occurs upon Ajuba depletion by siRNA, generating by itself conditions of induction in absence of DNA damage. The negative regulation exerted by Ajuba on the ATR pathway could occur by steric hindrance of the assembly of the ATR activating complex on RPA70. Dissociation of Ajuba or its depletion could free up the recruiting surface for the 9-1-1 complex, TOPBP1 or ATR-ATRIP and allow for spontaneous activation downstream. More work would be required to test this model, by asking whether binding of Ajuba to RPA70 is mutually exclusive with components of the ATR activation complex *in vitro*.

This leaves an important question: how can ATR be activated in the first place? We propose that activation conditions (such as hydroxyurea) lead to dissociation of Ajuba. What leads to this dissociation, or reduction of binding affinity of Ajuba for RPA70, remains to be elucidated. Phosphorylation of RPA32 could be an important event in this context, by preventing Ajuba from re-associating with the complex, or by promoting Ajuba dissociation from the complex, thereby reducing the occupancy of the activating platform on RPA70. Another

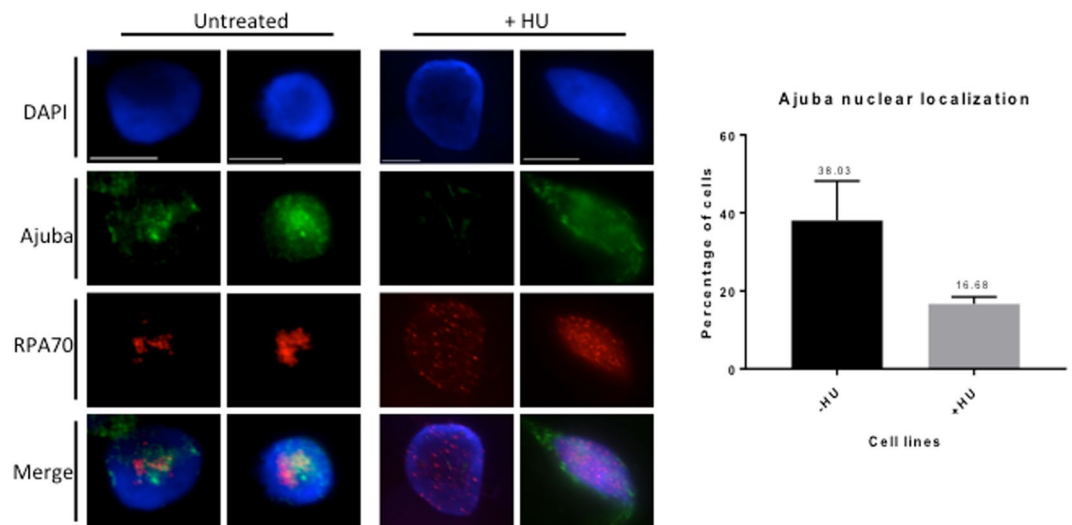


Figure 8. Ajuba nuclear localization is reduced upon HU treatment. (Left) Co-immunofluorescence of Ajuba (FITC) and RPA70 (TRITC) in untreated and HU treated HTC75 cells. (Right) Quantification of cells exhibiting strong nuclear localization with and without HU treatment (n = 100, three independent experiments).

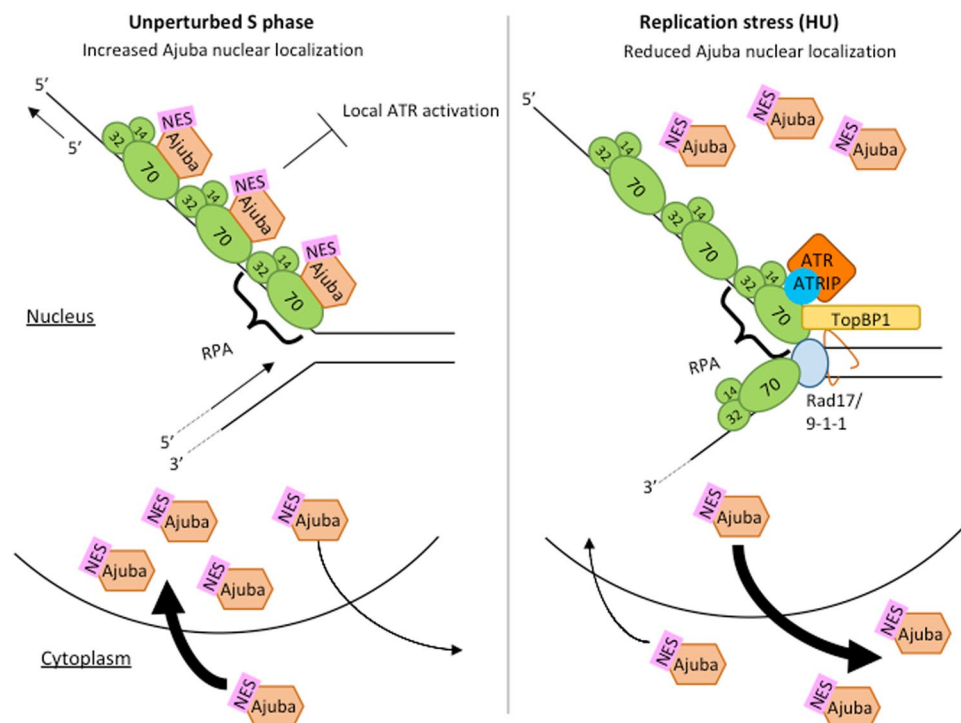


Figure 9. Model for Ajuba's function during unperturbed S phase and replication stress (induced by HU treatment). (Left) During unperturbed S phase, Ajuba nuclear localization increases, and Ajuba associates with the RPA heterotrimer in the nucleus through direct interaction with RPA70-OB fold A. This interaction inhibits local ATR activation at the replication site. (Right) During replication stress (induced by HU treatment), Ajuba dissociates from RPA and allows for the assembly of the ATR-inducing complex. Ajuba is shuttled out of the nucleus via its NES (nuclear export signal). ATR activation takes place at the specific site of damage, but not at other sites in the genome where Ajuba continues to exert its repressive activity.

possibility could be that DNA damage induces a posttranslational modification of Ajuba itself, resulting in a decrease in affinity for RPA. These are testable models for future studies. Finally, our model proposes that Ajuba is involved in local activation of the kinase, and is important to prevent a global response: it could explain activation of ATR at a single replication fork, or at a specific site of DNA damage in the genome, and how the response

is elicited locally, while kept at bay globally elsewhere in the genome. We propose that this type of regulation is essential to cell viability in order to impart the right dosage of a response essential to genome integrity, but which, when hyper-activated, would lead to cell death by apoptosis. Ajuba would then allow a “fine tuning” of the ATR response, by preventing the ATR pathway to be activated at places other than the actual site of damage and keeping the response locally constrained. It would be interesting to address whether Ajuba is implicated in other RPA-dependent responses, such as homology-directed repair, or interstrand crosslink repair²⁵.

Materials and Methods

Recombinant protein plasmid construction. For *in vitro* translations Ajuba and Trip6 was amplified using PCR with primers, Ajuba-HIS-5' and Ajuba-HIS-3', digested with EcoRI and XhoI, and cloned into pcDNA 3.1/His-B. RPA subunits were amplified with PCR using primers with EcoRI digestion sites and cloned into pCMV-TnT vector (Promega). RPA70-5' (5'-GTA TAT GAA TTC ATG GTC GGCCAA CTG AGC GAG-3'), RPA70-3' (5'-GTA TAT GAA TTC TCA CAT CAA TGC ACT TCT-3'), RPA32-5' (5'-GTA TAT GAA TTC ATG TGG AAC AGT GGA TTC GAA-3'), RPA32-3' (5'-GTA TAT GAATTC TTA TTCTGC ATC TGT GGA-3'), RPA14-5' (5'-GTA TAT GAATTC ATG GTG GAC ATG ATG GAC TTG-3'), RPA14-3' (5'-GTA TAT GAA TTC TCA ATC ATG TTG CAC AAT-3'). POT1 was amplified with PCR with primers containing XhoI digestion sequence into pCMV-TnT vector. POT1-5' (5'-GTA TCC TCG AGA TGT CTT TGG TTC CAG CAA C-3'), POT1-3' (5'-GTA TCC TCG AGT TAG ATT ACA TCT TC TGCA AC-3').

Ajuba truncation mutants were produced using PCR with primers containing EcoRI and XhoI digestion sites into pcDNA3.1-B/NT-His vector (Invitrogen). LIM-HIS, aa 337-538: LIM-HIS-5' (5'-CAC ACG AAT TCT GGC ACC TGT ATC AAG TGC AAC-3'), Ajuba-HIS-3'. PreLIM-HIS, aa 1-337: Ajuba-HIS-5', PreLIM-HIS-3' (5'-GTA CAC CTC GAG TCA GCC GAA GTA GTC CTC CCT GGC-3'). PreLIM/LIM1-HIS, aa 1-397: Ajuba-HIS-5', PreLIM/LIM1-HIS-3' (5'-GTA CAC CTC GAG TCA CTG AAA CCC TGA AAA CAG-3'). PreLIM/LIM12-HIS, aa 1-460: Ajuba-HIS-5', PreLIM/LIM1 + 2-HIS-3' (5'-GTA CAC CTC GAG TCA AGC ATA ATT TTT GTG GTA-3').

RPA70 truncation mutants were produced using PCR with primers containing EcoRI digestion sequences into pCMV-TnT vector. RPA70-OBABC, aa 169-612: OBABC-5' (5'-CAC AAC GAA TTC ATG GGT CCC AGC CTG TCA CAC-3'), RPA70-3'. RPA70-OBF, aa 1-169: RPA70-5', OBF-3' (5'-CAC AAC GAA TTC TCA TGC AGC TTT TCC AAA TGT CTT-3'). RPA70-OB + C, aa 302-612: OBBC-5' (5'-CAC AAC GAA TTC ATG GAT TTC ACG GGG ATT GAT GAC-3'), RPA70-3'. RPA70-OBF + A, aa 1-169: RPA70-5', OBF + A-3' (5'-CAC AAC GAA TTC TCA GAA ATC AAA CTG AAC CGT-3'). RPA70-OB½ABC, aa 234-612: OB½ABC-5' (5'-CAC AAC GAA TTC ATG CGA GCT ACA GCT TTC AAT-3'), RPA70-3'. Clones were confirmed by sequencing.

Cell culture. HTC75 and IMR90 (human diploid lung fibroblasts) (ATCC® CCL-186™) cell lines were employed. HTC75 is a derivative of HT1080 (human fibrosarcoma). IMR90 was used at population doubling 30. HTC75 cells were cultured in DMEM (Cellgro) with 10% BCS (HyClone), 1% penicillin and streptomycin (Cellgro) and 1% L-glutamine (Gibco). IMR90 cells were cultured in DMEM with 20% FBS (ClonTech), and 1% penicillin and streptomycin. Both cell lines were grown in cell culture incubator at 37°C with 5% CO₂.

Hydroxyurea treatment, BrdU staining and double thymidine block. Hydroxyurea (Thermo Scientific) was added to the medium to a final concentration of 2 mM. Cells were collected after 24 hours of treatment. The BrdU labeling was performed as per the manufacturer's protocol (ThermoFisher, cat. #B23151). Briefly, cells were grown in 6-well dishes and pulsed for 1 hour with 10 μM BrdU (from 10 mM stock). Cells were rinsed with PBS twice and grown further in regular medium, for asynchronous cultures. For cell cycle-staged cells, cells were synchronized first (see below), then pulsed for one hour with BrdU immediately after release. The detection was performed by immunofluorescence using a FITC-conjugated anti-BrdU antibody (eBioscience cat.# BU20A).

Double thymidine block was performed by adding 2 mM thymidine (final concentration) to the media. Cells were synchronized for 18 hours, rinsed with PBS, and fresh media was added to release for 10 hours. Thymidine (2 mM final concentration) was added the second time for 18 hours. Cells were rinsed with PBS and fresh media was added to release cells from G1/S border for hours indicated.

Co-Immunoprecipitation. Cell extracts preparation and protocol were carried out as described in (14)²⁶.

Co-immunofluorescence. HTC75 and IMR90 cells were grown on glass coverslips and were washed twice with PBS at room temperature. Nucleoplasmic proteins were extracted with Triton X-100 buffer at room temperature for 10 minutes. Cells were rinsed with PBS twice and fixed in 3% paraformaldehyde/2% sucrose in PBS for 10 minutes at room temperature. Cells were washed with Triton X-100 buffer for 10 minutes at room temperature and washed with PBS twice (5 minutes each), then blocked with PBG (0.2% cold water fish gelatin, Sigma G-7765, 0.5% BSA, Sigma A-2153, in PBS) for 30 minutes at RT. Added primary antibody diluted in PBG (Ajuba 1:2500, RPA70 1:2500) and stored at 4°C overnight. Coverslips were washed with PBG three times and incubated with fluorescent secondary antibody diluted in PBG for 45 minutes at RT (Anti-rabbit 1:1000, Anti-mouse 1:1000), then washed with PBG twice and incubated with DAPI in PBG at 100 ng/ml. Coverslips were mounted on microscope slides with embedding media and sealed with nail polish. Antibodies used: Ajuba (rabbit, Abcam #64451), RPA70 (mouse, Abcam #176467), PCNA (mouse, Santa Cruz).

***In vitro* co-translation.** 1 μg of Ajuba/Ajuba mutant plasmid and 1 μg of RPA subunit/RPA70/RPA70 mutant plasmid were added into the same reaction. The *in vitro* translation protocol was performed as described in manual from manufacturer (Promega, TNT® T7 Coupled Reticulocyte Lysate System) with 35S-methionine.

All proteins were co-translated in the same reaction tube, as in Figs 5–7, and the pull-down efficiency was much lower when proteins were translated separately before the binding assay (not shown).

His-tag affinity pulldown. Ni-NTA beads (BioRad, 156-0133) were washed with dH₂O and TBST (pH = 8.0, 0.01% Tween-20). The beads were blocked with 2% BSA (Sigma) (10 mg/ml) in TBST for 2 hours at room temperature. 20 ul of blocked beads were added to each sample and incubated at room temperature for 30 minutes. Beads were washed with 100 ul TBST six times and loading buffer was added directly to beads.

Autoradiography. SDS-PAGE gels were dried and placed for exposure into a phosphor storage cassette overnight (Amersham). The data was visualized and quantitated by Phosphor imager (Typhoon) using the ImageQuant software.

References

- Ciccia, A. & Elledge, S. J. The DNA damage response: making it safe to play with knives. *Mol Cell* **40**, 179–204 (2010).
- Zeman, M. K. & Cimprich, K. A. Causes and consequences of replication stress. *Nat Cell Biol* **16**, 2–9 (2014).
- Fernet, M., Chiker S. & Hall, J. ATM/ATR Cell Cycle Checkpoints: Mechanisms and Manipulation in Cancer Therapy in *DNA Repair and Cancer* (eds S. Madhusudan, & M. Wilson, III.) 426–469 (CRC Press, 2013).
- Vassin, V. M., Anantha, R. W., Sokolova, E., Kanner, S. & Borowiec, J. A. Human RPA phosphorylation by ATR stimulates DNA synthesis and prevents ssDNA accumulation during DNA-replication stress. *J Cell Sci* **122**, 4070–4080 (2009).
- Zou, L. Single- and double-stranded DNA: building a trigger of ATR-mediated DNA damage response. *Genes Dev* **21**, 879–885 (2007).
- Xu, X. *et al.* The basic cleft of RPA70N binds multiple checkpoint proteins, including RAD9, to regulate ATR signaling. *Mol Cell Biol* **28**, 7345–7353 (2008).
- Acevedo, J., Yan, S. & Michael, W. M. Direct Binding to Replication Protein A (RPA)-coated Single-stranded DNA Allows for Recruitment of the ATR Activator TopBP1 to Sites of DNA Damage. *J Biol Chem* **291**, 13124–13131 (2016).
- Liu, S. *et al.* ATR autophosphorylation as a molecular switch for checkpoint activation. *Mol Cell* **43**, 192–202 (2011).
- Wold, M. S. Replication protein A: a heterotrimeric, single-stranded DNA-binding protein required for eukaryotic DNA metabolism. *Annu Rev Biochem* **66**, 61–92 (1997).
- Lindsey-Boltz, L. A., Reardon, J. T., Wold, M. S. & Sancar, A. *In vitro* analysis of the role of replication protein A (RPA) and RPA phosphorylation in ATR-mediated checkpoint signaling. *J Biol Chem* **287**, 36123–36131 (2012).
- A. G., M. OB(oligonucleotide/oligosaccharide binding)-fold: common structural and functional solution for non-homologous sequences. *EMBO J* **12**, 861–867 (1993).
- Flynn, R. L. & Zou, L. Oligonucleotide/oligosaccharide-binding fold proteins: a growing family of genome guardians. *Crit Rev Biochem Mol Biol* **45**, 266–275 (2010).
- Flynn, R. L. & Zou, L. ATR: a master conductor of cellular responses to DNA replication stress. *Trends Biochem Sci* **36**, 133–140 (2011).
- Kalan, S., Matveyenko, A. & Loayza, D. LIM Protein Ajuba Participates in the Repression of the ATR-Mediated DNA Damage Response. *Front Genet* **4**, 95 (2013).
- Zheng, Q. & Zhao, Y. The diverse biofunctions of LIM domain proteins: determined by subcellular localization and protein-protein interaction. *Biol Cell* **99**, 489–502 (2007).
- Kadrmaz, J. L. & Beckerle, M. C. The LIM domain: from the cytoskeleton to the nucleus. *Nat Rev Mol Cell Biol* **5**, 920–931 (2004).
- Sheppard, S. A., Savinova, T. & Loayza, D. TRIP6 and LPP, but not Zyxin, are present at a subset of telomeres in human cells. *Cell Cycle* **10**, 1–5 (2011).
- Sheppard, S. A. & Loayza, D. LIM-domain proteins TRIP6 and LPP associate with shelterin to mediate telomere protection. *Aging (Albany NY)* **2**, 432–444 (2010).
- Goyal, R. K. *et al.* Ajuba, a novel LIM protein, interacts with Grb2, augments mitogen-activated protein kinase activity in fibroblasts, and promotes meiotic maturation of *Xenopus* oocytes in a Grb2- and Ras-dependent manner. *Mol Cell Biol* **19**, 4379–4389 (1999).
- Kanungo, J., Pratt, S. J., Marie, H. & Longmore, G. D. Ajuba, a cytosolic LIM protein, shuttles into the nucleus and affects embryonal cell proliferation and fate decisions. *Mol Biol Cell* **11**, 3299–3313 (2000).
- Schimizzi, G. V. & Longmore, G. D. Ajuba proteins. *Curr Biol* **25**, R445–6 (2015).
- Hervy, M., Hoffman, L. & Beckerle, M. C. From the membrane to the nucleus and back again: bifunctional focal adhesion proteins. *Curr Opin Cell Biol* **18**, 524–532 (2006).
- Wang, Y. & TD, G. LIM domain protein Trip6 has a conserved nuclear export signal, nuclear targeting sequences, and multiple transactivation domains. *Biochim Biophys Acta* **1538**, 260–272 (2001).
- Wang, Y. & Gilmore, T. D. Zyxin and paxillin proteins: focal adhesion plaque LIM domain proteins go nuclear. *BBA-Molecular Cell Research* **1593**, 115–120 (2003).
- Wang, W. Emergence of a DNA-damage response network consisting of Fanconi anaemia and BRCA proteins. *Nat Rev Genet* **8**, 735–748 (2007).
- Loayza, D. & de Lange, T. POT1 as a terminal transducer of TRF1 telomere length control. *Nature* **424**, 1013–1018 (2003).

Acknowledgements

This work was funded by a SC3 score award #1SC3GM094071-01A1 from the National Institute of General Medical Sciences. The authors thank Danielle Khan and Baila Schochet, both Hunter College undergraduates, for excellent technical assistance. S.F. was the recipient of the Inga Richter Fellowship, which provided invaluable support towards the completion of this work.

Author Contributions

Conception or design of the work: S.F., S.K., D.L. Data Collection: S.F., S.K., P.M. Analysis and Interpretation of the Data: S.F., S.K., P.M., D.L. Drafting the article: S.F., D.L. Figure preparation: S.F., D.L. All authors reviewed and approved the manuscript.

Additional Information

Supplementary information accompanies this paper at <https://doi.org/10.1038/s41598-018-27919-8>.

Competing Interests: The authors declare no competing interests.

Publisher's note: Springer Nature remains neutral with regard to jurisdictional claims in published maps and institutional affiliations.



Open Access This article is licensed under a Creative Commons Attribution 4.0 International License, which permits use, sharing, adaptation, distribution and reproduction in any medium or format, as long as you give appropriate credit to the original author(s) and the source, provide a link to the Creative Commons license, and indicate if changes were made. The images or other third party material in this article are included in the article's Creative Commons license, unless indicated otherwise in a credit line to the material. If material is not included in the article's Creative Commons license and your intended use is not permitted by statutory regulation or exceeds the permitted use, you will need to obtain permission directly from the copyright holder. To view a copy of this license, visit <http://creativecommons.org/licenses/by/4.0/>.

© The Author(s) 2018